

A Comprehensive Model for Single Ring Infiltration

II: Estimating Field-Saturated Hydraulic Conductivity

Ryan D. Stewart*

Dep. of Crop and Soil
Virginia Polytechnic Inst. and State Univ.
Environmental Science
Blacksburg, VA 24061

Majdi R. Abou Najm

Dep. of Civil and Environ. Engineering
American Univ. of Beirut
Beirut, Lebanon

In this study, we explored four approaches to infer field-saturated hydraulic conductivity (K_{fs}) from both early-time and steady-state infiltration measurements using an explicit expression for three-dimensional flow. All approaches required an estimate of the soil capillary length, λ . Approach 1 estimated K_{fs} via optimization, in which all other infiltration parameters (9 in total) were known. The remaining approaches constrained λ through different interpretations of coefficients generated by linear regression between infiltration and time. Approach 2 utilized these coefficients plus estimated soil water content to simultaneously quantify both λ and K_{fs} . Approach 3 used an analytical expression in which λ was estimated based on water retention/unsaturated hydraulic conductivity parameters, while Approach 4 adopted a universal λ value of 15 cm. The accuracy of these four approaches were tested using numerical and laboratory infiltration data. Approach 1 had the highest accuracy but also required the most auxiliary data, making it most suitable for laboratory and numerical experiments. Approach 2 was the least consistent, providing negative estimates for λ and K_{fs} under certain conditions. Approach 3 also gave accurate predictions of K_{fs} , but may be inaccurate in instances where the water retention model parameters are uncertain or do not describe soil hydraulic behaviors well. Approach 4 provided reasonable estimates of K_{fs} (within a factor of three from the actual value in most cases), while not requiring additional observational data. The optimal approach for interpreting K_{fs} will thus vary depending on the type and quality of available auxiliary data.

Infiltration tests are often used to determine soil physical properties such as field-saturated hydraulic conductivity, K_{fs} . In recent years, single ring infiltrometers have become widely utilized toward this goal, as they are typically easy to set up and conduct, require minimal water and time, and allow for multiple simultaneous measurements within close spatial proximity (Bagarello et al., 2014; Castellini et al., 2016; Stewart et al., 2015; Stewart et al., 2013).

Interpreting K_{fs} from three-dimensional infiltration data requires constraining the capillary force. In many solutions, the capillary force is represented by a length term, λ [L], or its reciprocal α^* [L^{-1}] (Bagarello et al., 2014; Reynolds et al., 2002a). This “capillary length” term (λ) can be quantified by using infiltration tests with multiple ring diameters (Scotter et al., 1982) or multiple source pressure heads (Reynolds et al., 2002a), by assuming a representative value based on soil textural class (Reynolds et al., 2002a), or by applying analytical expressions (as detailed in Part I of this study, Stewart and Abou Najm, 2018). Soil structural features such as aggregation and cracking often reduce the λ term (or conversely increases the α^* value), as detailed in Table 3.4-4 in Reynolds et al. (2002a). As a result, repacked or non-structured soil may have larger capillary length (λ) values compared with field soils, by up to one order of magnitude.

Once the capillary length has been constrained, infiltration measurements can be interpreted using early-time data (Wu et al., 1999), steady-state data (Reynolds and Elrick, 1990), or a combination of both (Part I of this study, Stewart and Abou Najm,

Core Ideas

- Four approaches were tested to estimate K_{fs} from single ring infiltration data.
- Highest accuracy occurred when capillary length was appropriately constrained.
- K_{fs} estimates improved if capillary length was overestimated vs. underestimated.
- Assuming a universal capillary length can also be useful for determining K_{fs} .
- K_{fs} can be accurately estimated using both early-time and steady-state data.

Soil Sci. Soc. Am. J. 82:558–567

doi:10.2136/sssaj2017.09.0314

Received 8 Sept. 2017.

Accepted 7 Feb. 2018.

*Corresponding author (ryan.stewart@vt.edu).

© Soil Science Society of America, 5585 Guilford Rd., Madison WI 53711 USA. All Rights reserved.

2018). Another procedure for analyzing single ring infiltration measurements is called the Beerkan Estimation of Soil Transfer properties, or BEST (Lassabatère et al., 2006). Full interpretation using the BEST method requires estimates of the initial and final water contents, bulk density, particle size distributions, wetting front depth, and lateral wetting distance. To simplify this process, Bagarello et al. (2014) used a constant capillary length value of $\alpha^* = 0.12$ cm for all soil types, which resulted in K_{fs} estimates that were within a factor of two of those predicted by the full BEST protocol for a set of agricultural soils. However, the model does not allow for differences in ring insertion depths or source pressures (i.e., ponded depths), and therefore may not work well with different experimental settings (e.g., positive water ponding heights in the single ring source).

In this study we explore four different approaches to determine K_{fs} from single ring infiltration measurements, using a comprehensive single ring infiltration model that was developed in Part I of this study (Stewart and Abou Najm, 2018). Each approach differs in how it constrains the capillary length, λ (a term that describes the capillary force driving early-time and three-dimensional water flow), and in terms of data requirements. The approaches can use both early-time and steady-state infiltration data, making them relevant to a range of test conditions. To illustrate how the proposed methods are suitable for most situations and experimental conditions, we applied them to evaluate infiltration tests for five simulated soils in HYDRUS and for laboratory tests in a sandy loam soil.

Theory

As established in Part I (Stewart and Abou Najm, 2018), cumulative infiltration I [L] can be described as a function of time t [T] as:

$$I = \sqrt{(\theta_s - \theta_i)(b_{source} + \lambda)K_{fs}/b} \sqrt{t} + afK_{fs}t \quad t < \tau_{crit} \quad [1a]$$

$$I = \frac{(\theta_s - \theta_i)(b_{source} + \lambda)}{4fb(1-a)} + fK_{fs}t \quad t \geq \tau_{crit} \quad [1b]$$

$$\tau_{crit} = \frac{(\theta_s - \theta_i)(b_{source} + \lambda)}{4bK_{fs}f^2(1-a)^2} \quad [1c]$$

where θ_i and θ_s are the respective initial (i.e., background) and saturated soil water contents, b_{source} is the pressure head at the single ring water source [L], λ is the capillary length [L], K_{fs} is

the field-saturated hydraulic conductivity [$L T^{-1}$], and a and b are constants (with assumed values of $a = 0.45$ and $b = 0.55$). f is a three-dimensional shape parameter defined by:

$$f = \frac{b_{source} + \lambda}{d + r_d/2} + 1 \quad [2]$$

where d is the depth of insertion of the single ring [L] and r_d is the disk radius of the ring [L].

Infiltration measurements, as interpreted using Eq. [1] and [2], can be used to estimate K_{fs} , so long as all other relevant parameters are known or constrained (Table 1). Operational parameters depend on the settings of each infiltration test, and so are relatively easy to quantify. In contrast, soil and conditional parameters vary between sites and situations. Here we summarize four different approaches that can be used for generating the necessary constraints to estimate K_{fs} .

Approach 1: Known λ , θ_i , and θ_s

In the first, simplest case, all parameters (Table 1) are known or constrained except for K_{fs} . Equation [1] can then be fit directly to the observed data (using the appropriate expression for the specific conditions of the infiltration test), for example by minimizing the residuals between the measurements and modeled data by adjusting the parameter value of K_{fs} . This approach requires the most auxiliary data, which can limit its applicability compared with the other approaches. On the other hand, this approach can be used with all data (i.e., early-time and steady-state conditions), whereas the other approaches require working with only one or the other.

Approach 2: Unknown λ , Known θ_i and θ_s

In the case of early-time data, that is, when $t < \tau_{crit}$, K_{fs} can be estimated by linearizing Eq. [1a]. For example, Smiles and Knight (1976) recommended dividing cumulative infiltration by $t^{1/2}$ to obtain, in the case of [1a]:

$$\frac{I}{t^{1/2}} = \sqrt{(\theta_s - \theta_i)(b_{source} + \lambda)K_{fs}/b} + afK_{fs}t^{1/2} = c_1 + c_2t^{1/2} \quad [3]$$

In a related approach, Vandervaere et al. (1997) proposed differentiating cumulative infiltration with respect to $t^{1/2}$ as:

$$\frac{dI}{dt^{1/2}} = \sqrt{(\theta_s - \theta_i)(b_{source} + \lambda)K_{fs}/b} + 2afK_{fs}t^{1/2} = c_1 + 2c_2t^{1/2} \quad [4]$$

Table 1. Parameters required to solve for cumulative infiltration, I [L], as a function of time, t [T], using Eq. [1]. Parameter values are controlled by soil properties (Type = Soil), operational settings (Type = Operational), or a combination of soil properties and operational settings (Type = Conditional).

Parameter	Description	Dimension	Type
θ_s	Saturated water content	[-]	Soil
θ_i	Initial water content	[-]	Soil
λ	Capillary length	[L]	Soil
K_{fs}	Field-saturated hydraulic conductivity	[$L T^{-1}$]	Soil
h_{source}	Water supply pressure head	[L]	Operational
d	Single ring insertion depth	[L]	Operational
r_d	Single ring disk radius	[L]	Operational
a	Early-time gravity flow constant	[-]	Conditional
b	Sorptivity constant	[-]	Conditional
f	Three-dimensional wetting shape factor	[-]	Conditional

In this manner, the constants c_1 and c_2 can be estimated from linear models fit using Eq. [3] or [4]. However, it should be noted that this approach can result in an ill-conditioned problem due to time appearing in both the first and second terms of the right-hand side of Eq. [1a] (Vandervaere et al., 2000). In such cases, a procedure established by Lassabatère et al. (2006), which combines results from both early time and steady-state measurements, may instead be more suitable. However, the Lassabatère et al. (2006) method requires knowledge of steady-state infiltration rates, and therefore may not be appropriate for short duration tests or tests in fine-textured soils (where a steady state may not be reached during reasonable amounts of time).

Nonetheless, for situations where the use of Eq. [3] or [4] provides appropriate estimates of c_1 and c_2 , then, given an estimate of the initial and saturated water contents (θ_i and θ_s), the field-saturated hydraulic conductivity and capillary length can be estimated as:

$$K_{fs} = \frac{c_2}{a} \frac{bc_1^2 / (\theta_s - \theta_i)}{d + r_d / 2} \quad [5]$$

$$\lambda = \frac{bc_1^2}{K_{fs}(\theta_s - \theta_i)} - h_{source} \quad [6]$$

In the case of steady-state data (when $t \geq \tau_{crit}$), K_{fs} can be found by fitting a line between I and t :

$$I = \frac{(\theta_s - \theta_i)(h_{source} + \lambda)}{4fb(1-a)} + fK_{fs}t = c_3 + c_4t \quad [7]$$

$$K_{fs} = \frac{c_4(d + r_d / 2)}{\lambda + h_{source} + d + r_d / 2} \quad [8]$$

$$\lambda = \frac{4c_3b(1-a)(h_{source} + d + r/2) - h_{source}(\theta_s - \theta_i)(d + r/2)}{(\theta_s - \theta_i)(d + r/2) - 4c_3b(1-a)} \quad [9]$$

Because τ_{crit} is not known a priori, it may at times be difficult to know whether to use Eq. [5] to [6] (early-time conditions) or Eq. [7] to [9] (steady-state conditions). One possibility is to check if the last three measurements of infiltration rate ($\Delta I / \Delta t$) are within some small error (e.g., $\pm 5\%$) of one another; if so, the test has probably reached steady-state conditions (Thomas et al., 2016). A second choice is to focus on the earliest measurements (e.g., the first five to ten readings) and utilize the early-time approximation.

Approach 3: Constrained λ

Here we focus on analytical solutions for constraining λ using soil water retention and unsaturated hydraulic conductivity models, noting that the appropriateness of such solutions will depend on ability of the retention/conductivity models to accurately characterize soil hydraulic behaviors. Using as an example the Brooks and Corey (1964) hydraulic model, in Part I (Stewart and Abou Najm, 2018) of this study we quantified λ as:

$$\lambda = \left(\frac{h_b \eta - h_i (h_b / h_i)^\eta}{1 - \eta} \right) \quad h_i < h_b \quad [10a]$$

$$\lambda = -h_i \quad h_i \geq h_b \quad [10b]$$

where h_i is the initial matric head of the soil [L] and η and h_b are water retention/unsaturated hydraulic conductivity parameters. In the case that the soil is initially dry (e.g., $h_i < h_b$), the capillary length attains a maximum value, λ_{max} :

$$\lambda_{max} = h_b \eta / (1 - \eta) \quad [11]$$

While Eq. [11] is strictly valid for the case that the initial matric head h_i is much smaller than the bubbling pressure h_b (i.e., initially dry soils), in practice it is approximately true over the range $-\infty < h_i < \sim 2h_b$ (as detailed in Part I of this study, Stewart and Abou Najm, 2018).

Once the capillary length has been constrained, K_{fs} can be estimated directly from the early-time c_2 term of Eq. [3] or [4] as:

$$K_{fs} = \frac{c_2}{a \left(\frac{h_{source} + \lambda}{d + r_d / 2} + 1 \right)} \quad [12]$$

or from the steady-state c_4 term of Eq. [7] as (Reynolds and Elrick, 1990):

$$K_{fs} = \frac{c_4}{\left(\frac{h_{source} + \lambda}{d + r_d / 2} + 1 \right)} \quad [13]$$

Approach 4: Assumed λ^*

Next, in the case that the capillary length cannot be experimentally or analytically constrained, a universal capillary length value, λ^* , may instead be assumed. We recommend a value of $\lambda^* = 15$ cm, which should fall within one order of magnitude of the true value for many real soils. As in Approach 3, constraining the capillary length as λ^* allows K_{fs} to be quantified from the early-time results as:

$$K_{fs} = \frac{c_2}{a \left(\frac{h_{source} + \lambda^*}{d + r_d / 2} + 1 \right)} \quad [14]$$

or from the steady-state results as (Reynolds and Elrick, 1990):

$$K_{fs} = \frac{c_4}{\left(\frac{h_{source} + \lambda^*}{d + r_d / 2} + 1 \right)} \quad [15]$$

Equation [14] is analogous to the abridged BEST procedure developed by Bagarello et al. (2014), in which the Haverkamp et al. (1994) model is simplified to:

$$K_{fs} = \frac{c_2}{0.467 \left(\frac{2.92}{r_d \alpha^*} + 1 \right)} \quad [16]$$

$\alpha^* [L^{-1}]$ is equivalent to λ^{-1} , with a universal value of $\alpha^* = 0.12 \text{ cm}^{-1}$ recommended for most field soils (Bagarello et al., 2014).

METHODS

Numerical Simulations with HYDRUS-3D

HYDRUS-3D (Version 2.05.0250) was used to simulate infiltration from a single ring source for five different soil types. The models were configured as an axisymmetric (x - z) plane of 100-cm radius by 200-cm depth, with 47,739 nodes in total. The single ring was modeled as having a 10-cm radius ($r_d = 10$ cm) and two depths of insertion: $d = 1$ cm and $d = 5$ cm. A constant head condition was set at the portion of the top boundary corresponding to the single ring, with pressure heads of $h_{\text{source}} = 0$ cm and $h_{\text{source}} = 25$ cm both tested, while the remaining upper boundary was set as a no-flux source. Five soils were simulated: Guelph loam; Yolo light clay; Grenoble sand; Columbia silt; and Silt loam G.E.3 soil. The Brooks and Corey hydraulic model was used; parameter values came from Fuentes et al. (1992), and are summarized in Table 2. Two initial conditions were modeled for each soil: dry ($h_i = -5000$ cm) and wet ($h_i = -50$ cm for the first four soils; $h_i = -130$ cm for the Silt loam G.E.3 soil). All infiltration events lasted 500 min in total.

The simulated infiltration rates were then used to calculate K_{fs} and λ (the latter when applicable). For Approach 1, a least-squares regression was used to optimize K_{fs} so that Eq. [1] best matched the cumulative infiltration predicted by HYDRUS. In this instance all parameters except for K_{fs} were assumed to be known, based on the input parameter values used for the HYDRUS simulations. λ was estimated with Eq. [10]. For Approach 2, I/\sqrt{t} was plotted against \sqrt{t} (i.e., Eq. [3]) for the infiltration data corresponding to $t < \tau_{\text{crit}}$ and I against t (i.e., Eq. [7]) for any data corresponding to $t \geq \tau_{\text{crit}}$. Linear models were then fit to the data using a least-squares regression. The coefficients c_1 and c_2 were found from the early-time data (Eq. [3]), and the coefficients c_3 and c_4 came from the steady-state data (Eq. [7]). Those coefficients were then used to determine K_{fs} and λ via Eq. [5] to [9]. We assumed that $a = 0.45$ and $b = 0.55$, and used the input/modeled values for h_{source} , d , r_d , θ_i and θ_s .

We also examined the ability of the simplified expressions of Eq. [12] to [15] to constrain K_{fs} from infiltration measurements. For Approach 3, the input parameter values for h_b and η were used in Eq. [11] to calculate the capillary length λ_{max} for each soil, while in Approach 4 a universal value of $\lambda^* = 15$ cm was assumed for all soils. Finally, the Bagarello et al. (2014) model was fit to the c_2 estimates, using Eq. [16] and a constant value of $\alpha^* = 0.12 \text{ cm}^{-1}$.

Laboratory Tests

In addition to the numerical simulations, we performed two single ring infiltration tests in an air-dry fine sandy loam soil (Adkins series). The soil was collected from a farm near Echo, OR, and was repacked into a 50-cm diameter by 90-cm tall plastic barrel to a bulk density of approximately 1.58 Mg m^{-3} . The packed soil was 50 cm deep at the time of testing. To conduct the tests, we inserted a 9.6-cm diameter ABS plastic ring (1-cm wall thickness) into the material to a depth of 5 cm. We added water to the ring in 100 cm^3 increments for a total volume of 1600 cm^3 , recording the time required for each volume of water to infiltrate. The two tests were positioned within the barrel such that lateral extent of the wetting bulbs (as estimated at the surface) neither overlapped nor reached the sides of the container. As part of the experiment, nine intact soil cores (5.4 cm inner diameter by 3 cm length) were collected from the column and were saturated before being placed into a pressure plate system (Soilmoisture, Inc., Santa Barbara, CA). Soil water retention measurements were made on the cores at 0, 330, 660, and 1000 cm pressure heads. Soil θ_s was determined based on the water content of the saturated cores, and θ_r was based on the water content of the cores when air dry. A least-squares regression on the Brooks and Corey water retention model (Eq. [10] in Part I, Stewart and Abou Najm, 2018) was used to determine the parameters η and h_b . After collecting the experimental data, K_{fs} values for each test were estimated using the four approaches. The following parameter values were used (when applicable): $h_{\text{source}} = 0.5$ cm, $d = 5$ cm, $r = 4.8$ cm, $a = 0.7$, $b = 0.55$, and $\theta_i = \theta_r$.

Laboratory Test Validation

For validation, saturated hydraulic conductivity of the sandy loam soil was quantified using two additional approaches. For the first validation, we estimated K_{fs} and the water retention parameters η and h_b using the inverse model feature of HYDRUS-3D (Simunek and Sejna, 2011). The sand column was modeled as a 2D axisymmetric plane with a depth of 50 cm and a radius of 25 cm. Node spacing ranged from 0.25 cm in the vicinity of the ring to 1 cm at the far bottom edge of the domain. In total, 3874 nodes and 7499 elements were modeled. The ring was modeled using a no-flux domain for the perimeter in contact with the sand. The infiltration tests were simulated using a constant head of 0.5 cm for the upper portion of the boundary corresponding to the inside of the ring, while a no-flux boundary was used for the remaining sides. The initial pressure head was set to $h_i = -5,000$ cm. The initial soil properties

Table 2. Saturated water content (θ_s), residual water content (θ_r), saturated hydraulic conductivity (K_s), bubbling pressure head (h_b), and pore size index (η) for the soils used in comparisons and analysis.

No.	Soil	θ_s	θ_r	K_s cm min ⁻¹	h_b cm	η
1	Guelph loam	0.52	0.17	0.022	-45.82	3.56
2	Yolo light clay	0.50	0.0	0.00074	-16.56	2.62
3	Grenoble sand	0.31	0.0	0.26	-11.43	5.86
4	Columbia silt	0.40	0.0	0.0035	-6.657	5.45
5	Silt loam G.E.3	0.40	0.013	0.0035	-128.48	3.16

were set as: $\theta_r = 0.0138$, $\theta_s = 0.404$, $\eta = 3.183$, $h_b = -9.49$ cm, $K_{fs} = 0.05$ cm s⁻¹, and l (a tortuosity parameter) = 0.5. The model then optimized values for η , h_b and K_{fs} using the least-squares inverse solution routine based on the observed cumulative infiltration data; η was constrained to be between 2.6 and 6.5, to ensure model numerical stability.

For the second validation, constant head flow experiments were performed on three cylindrical cores (5.4 cm inner diameter by 3 cm length) collected from the soil. Flow measurements were conducted within sealed tempe cells (Soilmoisture, Inc., Santa Barbara, CA), following the procedure of Klute and Dirksen (1986). Hydraulic head loss across the cores was measured using a differential pressure transducer (Dwyer 2025 Magnehelic, Michigan City, IN). Note that because these cores were saturated (and thus theoretically did not contain entrapped air), they may represent an “end-member” of the maximum possible hydraulic conductivity that the soil can possess.

Statistical Analysis

For the numerical simulations, parameter estimates were assessed using the differences (%) between the actual values for λ (based on Eq. [10]) and K_{fs} (based on HYDRUS inputs), where the difference equals:

$$100 \times (\lambda_{\text{estimated}} - \lambda_{\text{actual}}) / \lambda_{\text{actual}} \quad [17]$$

and

$$100 \times (K_{fs,\text{estimated}} - K_{fs,\text{actual}}) / K_{fs,\text{actual}} \quad [18]$$

With this convention, values of -50% and +100% both represent a factor of two difference between estimated and actual parameter values, and -75% and +300% both represent a factor of four difference.

For the laboratory data, model fit was assessed using the root mean square deviation (RMSD), calculated as:

$$\text{RMSD} = \sqrt{\sum_{i=1}^N (\hat{y}_i - y_i)^2 / n} \quad [19]$$

where \hat{y}_i is the cumulative infiltration predicted by the proposed model at time i , y_i is the measured cumulative infiltration at time i , and n is the number of observations.

Sensitivity Analysis

We performed a sensitivity analysis to determine the effect of erroneous λ values on K_{fs} estimates. To conduct this analysis, we assessed how changes in λ affected subsequent estimates of K_{fs} . The baseline scenario assumed that $a = 0.45$, $d = 5$ cm, $r_d = 5$ cm, $c_2 = 0.00315$ cm s⁻¹, and $K_{fs} = 0.00125$ cm s⁻¹ (though note that the solution is insensitive to the actual values of a and c_2). The analysis then assumed that for all instances $\lambda_{\text{estimated}} = 19.6$ cm and $K_{fs,\text{estimated}} = 0.00125$ cm s⁻¹, whereas the “actual” λ value varied plus or minus an order of magnitude from the estimated value (i.e., $0.1 \leq (\lambda_{\text{actual}} / \lambda_{\text{estimated}}) \leq 10$). The corresponding relative changes in the “actual” value of K_{fs} relative to its estimated value (i.e., $K_{fs,\text{actual}} / K_{fs,\text{estimated}}$) were then analyzed for the baseline and six other combinations of ring radius (r_d) and ring insertion depth (d). The seven scenarios were: (i) $r_d = 5$ cm, $d = 5$ cm; (ii) $r_d = 5$ cm, $d = 2.5$ cm; (iii) $r_d = 2.5$ cm, $d = 5$ cm;

(iv) $r_d = 2.5$ cm, $d = 2.5$ cm; (v) $r_d = 5$ cm, $d = 10$ cm; (vi) $r_d = 10$ cm, $d = 5$ cm; and (vii) $r_d = 10$ cm, $d = 10$ cm. The analysis was repeated for two water supply pressure heads: $h_{\text{source}} = 0.5$ cm and $h_{\text{source}} = 25$ cm.

RESULTS AND DISCUSSION

Numerical Simulations

HYDRUS-3D was used to simulate infiltration into five synthetic soils (Guelph loam, Yolo light clay, Grenoble sand, Columbia silt, and Silt loam G.E.3). Approaches 2 to 4 were first used to estimate the capillary length (λ) values associated with the HYDRUS simulations (Fig. 1; Supplemental Table S1). Approach 2, which used the intercept of linearized infiltration data (i.e., as seen in Eq. [3], [4], or [7]), had relatively low accuracy, with most of the predicted λ values varying from those values calculated by Eq. [10] by more than a factor of two. In addition, six of the eighteen applicable simulations (33%) produced negative estimates for λ when analyzed using Eq. [9] for their steady-state data. This poor performance may be attributed to uncertainty in the c_3 term of Eq. [7]. Approach 3, which used water retention data to constrain λ_{max} was the most accurate, and only diverged from the λ estimated by Eq. [10] for three of the five soils in the initially wet conditions, with total differences less than 50% in all cases. The universal value of $\lambda^* = 15$ cm, which was used in Approach 4, varied by -92 to 84% from the λ values given by Eq. [10] (with the -92% difference corresponding to an approximately 12-fold underestimation, and the 84% difference corresponding to an approximate twofold overestimation).

Next, the four approaches, plus the Bagarello et al. (2014) method, were used to estimate K_{fs} based on the HYDRUS simulations. Approach 1, in which K_{fs} was estimated via parameter optimization, was the most accurate, with predicted K_{fs} values that varied from actual by 0 to 20% (Fig. 2; Supplemental Table S2). However, Approach 1 required constraining all parameters besides K_{fs} , making this method most suitable for numerical or laboratory exercises. Uncertainty in any of the terms, λ for example, would also render this approach less accurate (as discussed in the next section below).

Approach 2 provided the worst estimates of K_{fs} (Fig. 2; Supplemental Table S2), with differences that ranged from 4 to 1760% for the early-time data (Eq. [5]) and from 7 to 322% for the steady-state data (Eq. [8]). The negative λ values calculated by Eq. [9] translated to negative estimates of K_{fs} , again affecting six of the steady-state simulations. Altogether, when using Approach 2, any inaccuracies in estimating λ will compromise the ability of that method to estimate K_{fs} .

Approach 3, in which λ_{max} was constrained using water retention data (Eq. [10]), provided relatively accurate estimates of K_{fs} . The early-time data, analyzed using Eq. [12], predicted K_{fs} values that varied from actual by 2 to 129%, with all but one value differing from the true K_{fs} by less than 100% (Fig. 2; Supplemental Table S3). The steady-state data (analyzed with Eq. [13]) provided a similar range of 0 to 109%, with all but two values varying from actual by less than 35% (Fig. 2; Supplemental Table S3).

Approach 4, in which the capillary length was fixed at a universal value of $\lambda^* = 15$ cm, also provided fairly accurate predictions for K_{fs} for the Guelph loam, Yolo light clay, Grenoble sand and Columbia silt soils, varying from actual values by a factor of three or less for most combinations of initial pressure head (h_i), ring insertion depth (d), and water ponding depth h_{source} (Fig. 2; Supplemental Table S3). However, this approach was highly inaccurate for Silt loam G.E.3 soil (differences of 49 to 766%. This large error was likely due to the relatively large capillary length value of that soil ($\lambda_{actual} = 130$ to 188 cm), which means that the assumption of a universal value may be less accurate in fine-textured soils with large bubbling pressure and capillary length values. However, fine-textured soils tend to have lower capillary length values when in field conditions as compared with (re-packed) laboratory settings (Reynolds et al., 2002a). Further, Approach 4 required no additional information to interpret, and thus may make a good option for infiltration tests that are done

at high spatial resolutions (e.g., multiple measurements conducted within one or more fields) and/or repeated through time.

Approach 4 also compared well with the simplified BEST method proposed by Bagarello et al. (2014), with Approach 4 providing similar or smaller relative differences between predicted and actual K_{fs} values compared with the Bagarello et al. model (Fig. 2; Supplemental Table S3). Even though the Bagarello et al. model (Eq. [16]) does not explicitly account for ring depth, its K_{fs} estimates tended to be better for the $d = 5$ cm simulations than the $d = 1$ cm ones. This result could reflect the uncertainty in the assumed values for various constants (e.g., the proportionality constant γ) used in that analysis.

Overall, Approach 3, which only requires an estimate of the capillary length, may be the best method for use in field situations, assuming that λ is appropriately constrained. Approach 2, which estimates λ and K_{fs} from the infiltration data, was the most inaccurate and limiting (e.g., negative estimates for those

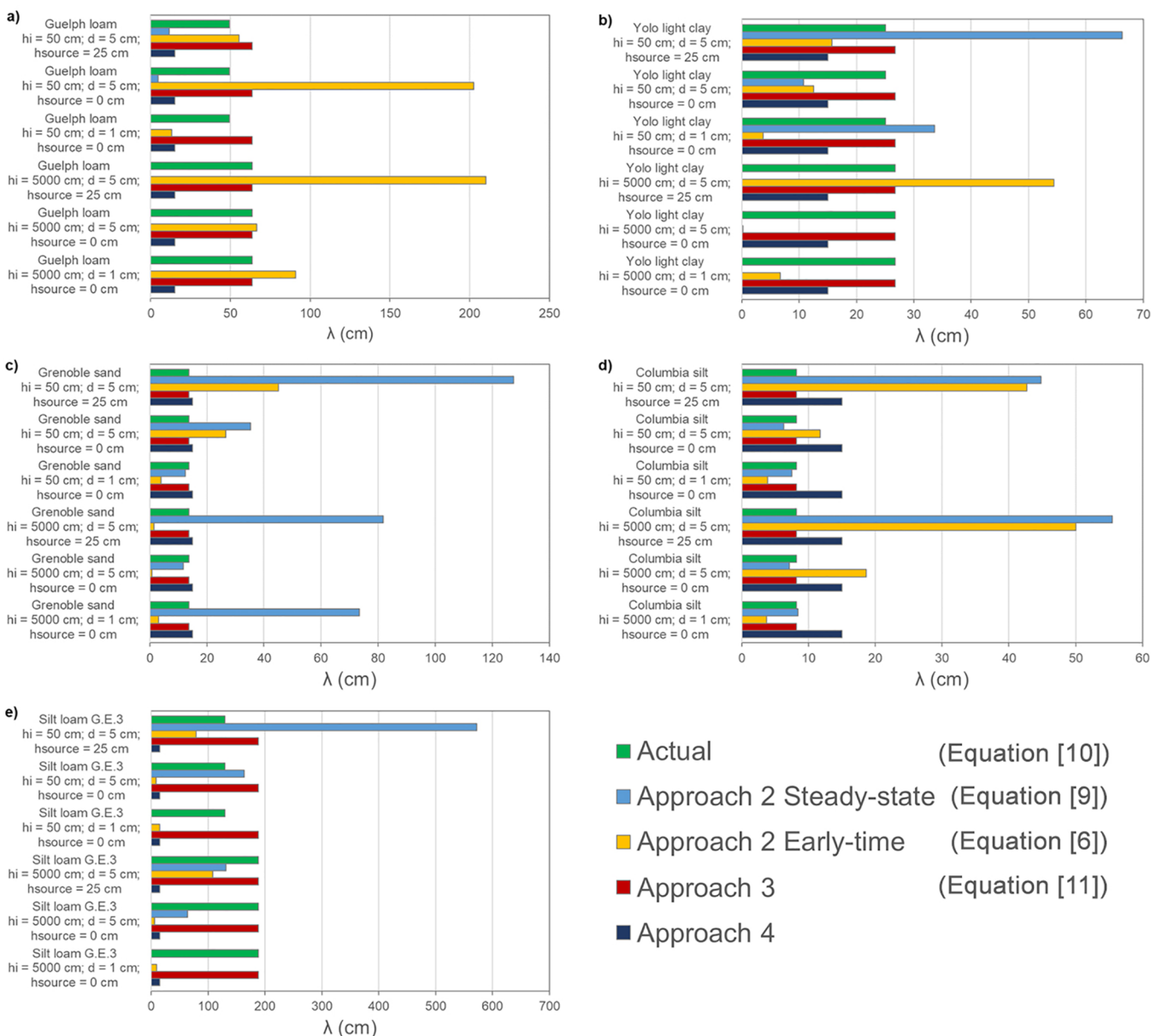


Fig. 1. Estimated capillary length (λ) for (a) Guelph loam; (b) Yolo light clay; (c) Grenoble sand; (d) Columbia silt; and (e) Silt loam G.E.3 soils.

parameters in some cases). Approach 2 also requires an estimate for change in volumetric water content that occurs during the infiltration event, which may not always be available or accurate in field settings. Thus, based on these results we recommend the use of Approaches 3 or 4 over Approach 2.

Laboratory Tests

Fitting the Brooks and Corey model to the water retention data using a least-squares regression resulted in parameter values of $h_b = 13.7$ cm and $\eta = 3.42$ (Fig. 3a). Putting those values into Eq. [11], we determined that $\lambda_{max} = 19.3$ cm (a value close to the recommended universal value of 15 cm; Fig. 3b). However, it should be noted that with only three observed water retention points, the optimized values can have considerable uncertainty.

The water retention parameters η and h_b , along with K_{fs} , were also estimated using a HYDRUS-3D inverse model based on two single ring infiltration tests done in the repacked Adkins sandy loam soil. The estimated water retention parameters through the HYDRUS optimization were $\eta = 4.40$ and $h_b = 34.7$ cm (Test 1) and $\eta = 4.75$ and $h_b = 34.4$ cm (Test 2). Using Eq. [11], the parameter combinations correspond to λ_{max} values of 44.7 cm (Test 1) and 43.5 cm (Test 2). Thus, the HYDRUS model predicted λ values that were approximately 2.5-fold greater than those estimated by the water retention measurements (Fig. 3b). Approach 2, in which λ was estimated based on Eq. [6], provided estimates that varied by nearly an order of magnitude between Tests 1 and 2. This result reiterates the considerable uncertainty seen when using Approach 2 during the numerical simulations.

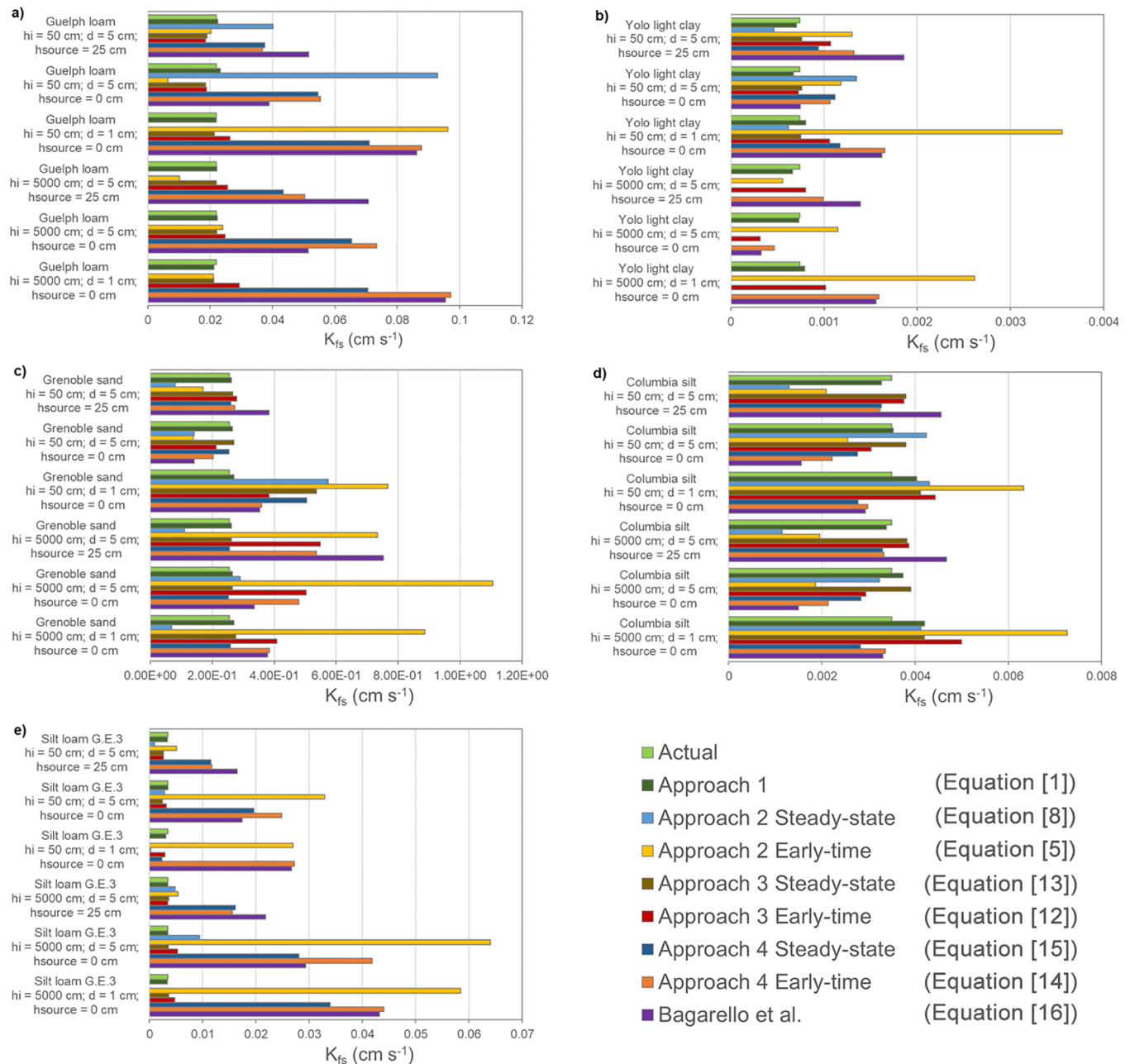


Fig. 2. Estimated field-saturated hydraulic conductivity (K_{fs}) in cm s^{-1} for a) Guelph loam; b) Yolo light clay; c) Grenoble sand; d) Columbia silt; and e) Silt loam G.E.3 soils.

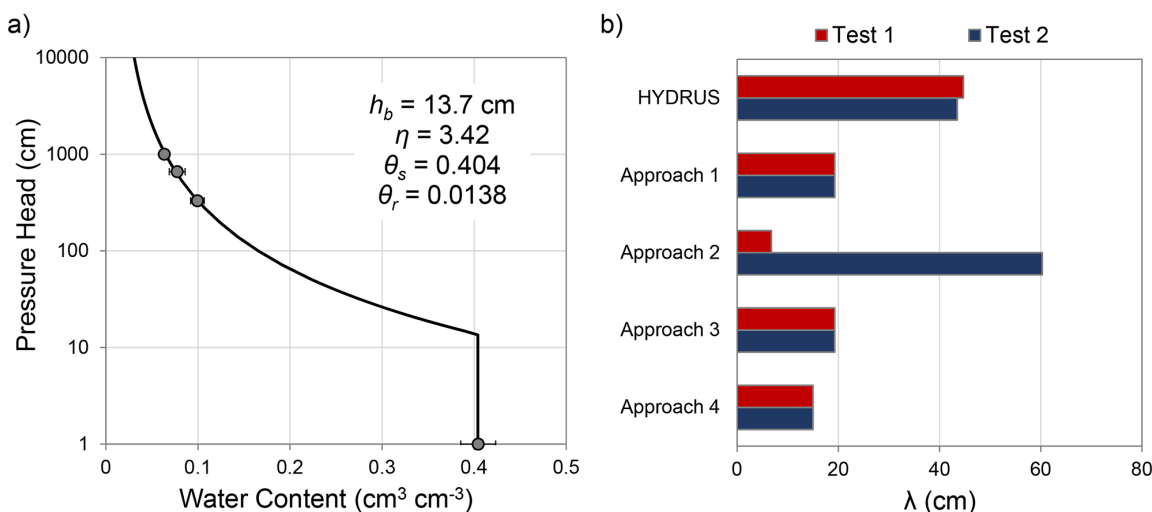


Fig. 3. (a) Measured water retention from an Adkins fine sandy loam soil fit with the Brooks and Corey hydraulic model ($n = 9$; error bars indicate the standard deviation); and (b) capillary length (λ) estimated from two laboratory infiltration tests using the inverse solution for HYDRUS-3D (“HYDRUS”), and the four analytical approaches (Approaches 1 to 4).

Next, K_{fs} was estimated using the four theoretical approaches, and those values were compared with “validation” data collected via the HYDRUS-3D inverse model and via permeability measurements taken on saturated cores. Approach 1 (assuming $\lambda = 19.3$ cm) gave optimized K_{fs} values of $1.91 \times 10^{-3} \text{ cm s}^{-1}$ (Test 1) and $2.60 \times 10^{-3} \text{ cm s}^{-1}$ (Test 2), with corresponding RMSD values of 0.33 cm and 0.38 cm when fitting Eq. [1] to the observed infiltration data (Fig. 4a, solid lines). The optimized HYDRUS model estimated K_{fs} values of $7.91 \times 10^{-4} \text{ cm s}^{-1}$ (Test 1) and $1.09 \times 10^{-3} \text{ cm s}^{-1}$ (Test 2). Compared with Eq. [1], the optimized HYDRUS models had relatively high RMSD values of 0.94 cm (Test 1) and 1.4 cm (Test 2), and did a relatively poor job of predicting early-time cumulative infiltration (Fig. 4a, dashed lines).

The remaining three theoretical approaches (i.e., Approaches 2 to 4) all predicted K_{fs} values that within a factor of 2 to 4 of Approach 1 (Fig. 4b; Supplemental Table S4). Three of the

four approaches predicted that the K_{fs} value associated with Test 2 was slightly larger than that of Test 1. Approach 2, conversely, estimated that the K_{fs} value associated with Test 1 was four times larger than that associated with Test 2, reflecting the uncertainty in capillary length values associated with that approach.

The constant head tests performed on the triplicate soil cores gave a mean K_{fs} value of $0.061 \pm 0.018 \text{ cm s}^{-1}$, which was 1 to 2 orders of magnitude higher than the K_{fs} estimates determined from the infiltration data (Fig. 4b). Soil cores often can have higher hydraulic conductivities than larger-scale (e.g., undisturbed field) soils (Reynolds et al., 2000, Stewart et al., 2016), due to effects such as preferential pathways that can bisect relatively short cores (Bouma, 1980) and flow along the core walls (Reynolds et al., 2000). At the same time, the permeability analyses performed on the soil cores likely reflected the saturated hydraulic conductivity (K_s) of the medium, while the infiltration tests (and inverse modeling done on those data) likely represented the field-saturated

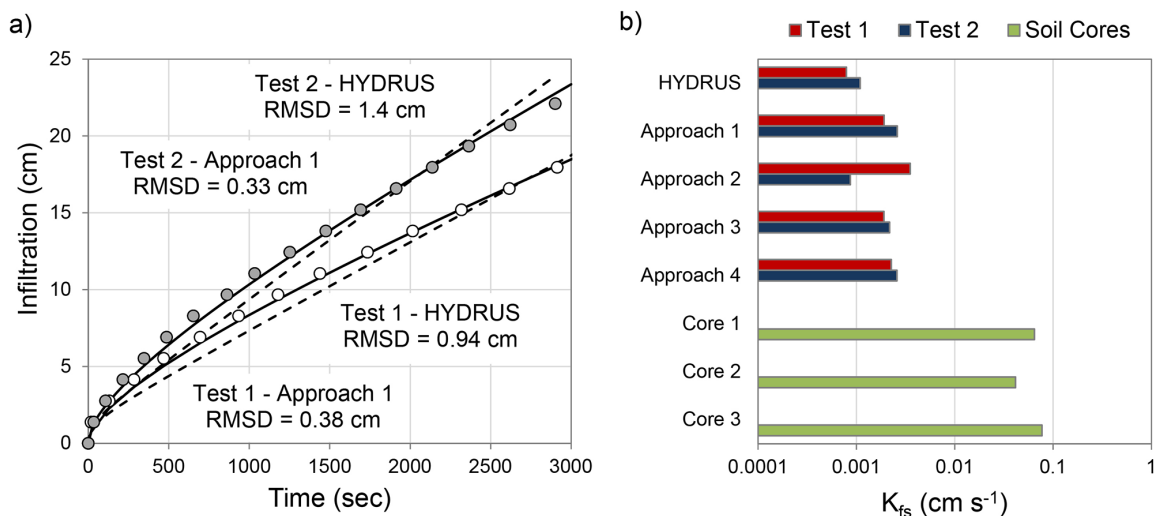


Fig. 4. (a) Observed (points) versus modeled (solid lines, Eq. [1]; dashed lines, inverse solution from HYDRUS-3D) cumulative infiltration for two single ring tests in the Adkins fine sandy loam; and (b) estimated field-saturated hydraulic conductivity (K_{fs}) from HYDRUS-3D and the four analytical Approaches 1 to 4. K_{fs} was also estimated from saturated constant head flow measurements performed on soil cores (Cores 1 to 3).

hydraulic conductivity (K_{fs}). Previous work has suggested that K_s and K_{fs} can vary by factors of 2 to 5 or more (Constantz et al., 1988, Reynolds et al., 2002b), so some of the discrepancy between the saturated cores and infiltration data may be attributable to factors such as entrapped air in the infiltration tests.

Sensitivity of K_{fs} Estimates to λ

While Approach 3 yielded good estimates of K_{fs} when λ_{max} was accurately quantified, uncertainty in λ may translate to error in K_{fs} . For instance, in the HYDRUS simulations, the water retention parameters were explicitly known, which allowed for accurate calculation of the capillary length λ (using Eq. [10] or [11]) and good estimates of K_{fs} (using Approach 3). However, in the laboratory study, the water retention function was parameterized using only three non-saturated points (Fig. 3). The lack of higher resolution data meant that multiple combinations of the parameters h_b and η could yield reasonable fits to the data, such as the combinations of $h_b = 78$ cm and $\eta = 4.79$; $h_b = 13.6$ cm and $\eta = 3.42$; and $h_b = 1.36$ cm and $\eta = 2.89$. The calculated λ values for those combinations ranged from 2.08 to 98.6 cm, or 1.5 orders of magnitude (corresponding, it should be noted, to the approximately 1.5 orders of magnitude difference between $h_b = 1.36$ cm and $h_b = 78$ cm).

Based on the potential uncertainty in estimates of h_b and λ , we performed a sensitivity analysis to determine the effect of errors in constraining λ on the subsequent estimation of K_{fs} . As seen in Fig. 5, errors in λ correspond to errors in K_{fs} , though the relationship is less than 1:1 (in other words, a twofold error in λ results in a less than twofold error in K_{fs}). The error in K_{fs} becomes reduced as the ring radius and insertion depth increase, as both of those terms affect the extent of three-dimensional wetting from a single ring source. Likewise, raising the water ponding depth (h_{source}) also reduces error, as increasing the hydrostatic pressure elevates

the relative contribution of gravity flow to capillary flow, thus improving the sensitivity of the measurement to K_{fs} (Reynolds et al., 2002a). Figure 5 also shows that K_{fs} estimates are more sensitive to underpredictions of λ (i.e., $\lambda_{actual}/\lambda_{estimated} > 1$) compared with overpredictions (i.e., $\lambda_{actual}/\lambda_{estimated} < 1$). For example, with $h_{source} = 25$ cm, a 10-fold overestimation of $\lambda_{actual}/\lambda_{estimated}$ would cause a ~ 1.5 -fold error in K_{fs} , whereas a 10-fold underestimation of $\lambda_{actual}/\lambda_{estimated}$ could cause K_{fs} to be underestimated by more than 4-fold (Fig. 5b). Thus, it appears to be preferable to overestimate rather than underpredict the value of λ . This effect may be a reason that Approach 4 had relatively better predictions of K_{fs} compared with the Bagarello et al. (2014) approach: in Approach 4, we assumed a capillary length value of $\lambda^* = 15$ cm, which is roughly twice as large as the equivalent α^* parameter used by Bagarello et al. (2014) (assuming $\alpha^* = 0.12$ cm $^{-1}$, which is equivalent to $\lambda = 8.3$ cm).

This analysis also highlights the potential drawback of Approach 3 if the water retention parameters and capillary length are not appropriately constrained. Given that overpredicting λ results in relatively less error in estimating K_{fs} than underpredicting λ , one potential solution when dealing with uncertain values for η and h_b is to use the greater of λ_{max} (from Eq. [11]) or $\lambda^* = 15$ cm. This analysis also suggests that a larger value of λ^* may be advisable when dealing with fine-textured soils, particularly when they are lacking in structural features (e.g., repacked samples).

Early-Time versus Steady-State Data

The numerical simulations allowed for comparison for K_{fs} estimates generated using early-time versus steady-state data. On one hand, the steady-state data provided more non-physical (negative) K_{fs} estimates than the early-time data, though such results were limited to Approach 2. At the same time, steady-state conditions were not reached during the 500-min simulations for the Yolo light clay in initially dry conditions, thus precluding the use of

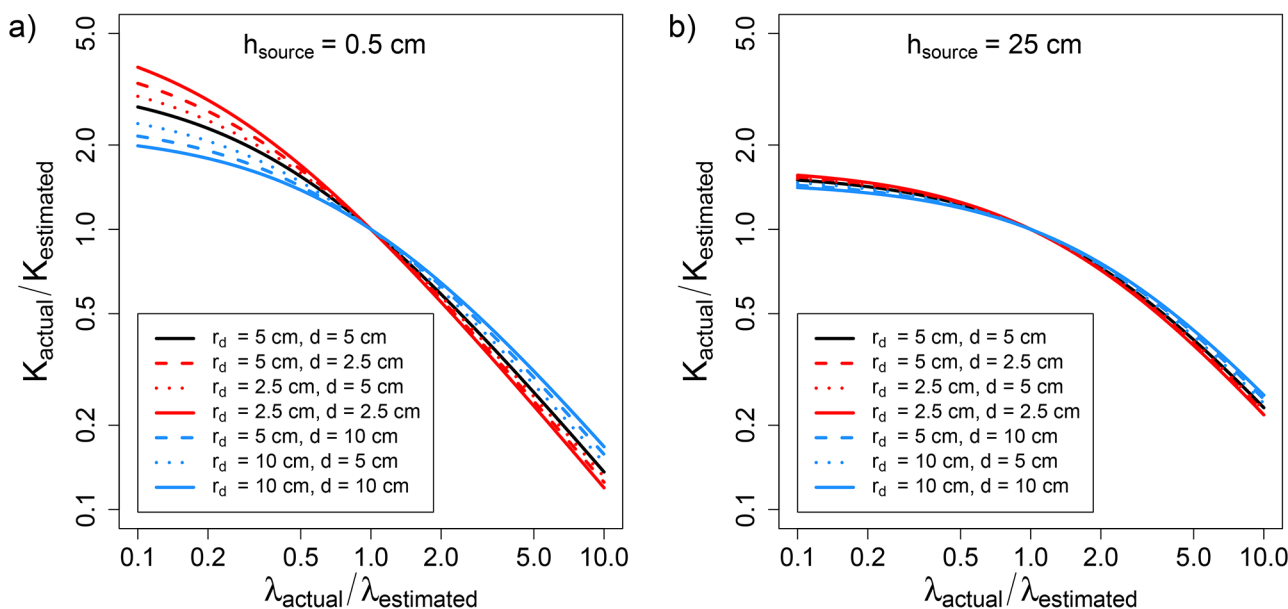


Fig. 5. Sensitivity of K_{fs} estimates ($K_{actual}/K_{estimated}$) from Eq. [12] based on error in properly constraining the capillary length term ($\lambda_{actual}/\lambda_{estimated}$). Combinations of three different disc radii (r_d) and ring insertion depths (d) were compared; $\lambda_{estimated}$ was set equal to 19.6 cm and h_{source} was set as (a) 0.5 cm and (b) 25 cm.

steady-state data. Finally, using the early-time data also can increase the speed of each test, which can be important when performing multiple tests. On the other hand, when using Approaches 3 or 4 (which we note are variations on the original Reynolds and Elrick (1990) analysis for steady-state flow), the steady-state infiltration data often provided more accurate estimates of K_{fs} than the early-time (transient) data. Thus, if experimental conditions allow, it may be preferable to use the steady-state data, either on its own or in combination with the early-time results.

SUMMARY AND CONCLUSIONS

In this study, we explored four methods for estimating field-saturated hydraulic conductivity (K_{fs}) from single-ring infiltration data using a generalized three-dimensional infiltration model. Using a comprehensive model means that hydraulic conductivity can be estimated from both early-time and steady-state infiltration data, thus increasing the range of conditions over which it can be applied. The most accurate results were obtained when the capillary length λ , which controls the sorptivity and three-dimensional wetting aspects of infiltration, was properly constrained. While λ can be experimentally determined using multiple ring diameters or multiple ponding depths (Reynolds et al., 2002a), here we explored quantifying λ using the water retention properties of the soil, such as the parameters b_b and η for the Brooks and Corey hydraulic model. This particular method was accurate so long as the soil was well described by the hydraulic model, whereas uncertainty in parameters such as b_b and η could potentially cause estimation errors for λ and K_{fs} . Still, a sensitivity analysis showed that K_{fs} was relatively insensitive to errors in λ , particularly as water supply pressure (h_{source}) increased. A uniform capillary length value of $\lambda^* = 15$ cm may therefore be applicable to many soils with acceptable accuracy, with less than twofold differences between estimated and actual K_{fs} found for the majority of soils and scenarios tested here. Using a uniform capillary length value means that no additional information is needed to estimate K_{fs} from single ring tests, which is particularly useful when conducting and interpreting numerous infiltration measurements.

ACKNOWLEDGMENTS

We would like to acknowledge Chadi Sayde and Javier Benítez-Buelga for performing the water retention experiment on the Adkins fine sandy loam soil. Funding for this work was provided by the USDA–NRCS Conservation Innovation Grant No. 69-3A75-14-260. Funding was also provided in part by the USDA–NRCS Virginia Agricultural Experiment Station and the Hatch Program of the USDA National Institute of Food and Agriculture.

SUPPLEMENTAL MATERIAL

Supplemental material is available with the online version of this article. The supplemental document presents in tabular form the estimated λ values (Approaches 2 to 4) and K_{fs} values (Approaches 1 to 4), along with the relative differences from actual values, from data obtained through the HYDRUS-3D simulations.

REFERENCES

Bagarello, V., S. Di Prima, M. Iovino, and G. Provenzano. 2014. Estimating field-saturated soil hydraulic conductivity by a simplified Beerkan infiltration experiment. *Hydrol. Processes* 28:1095–1103. doi:10.1002/hyp.9649

- Bouma, J. 1980. Field measurement of soil hydraulic properties characterizing water movement through swelling clay soils. *J. Hydrol.* 45:149–158. doi:10.1016/0022-1694(80)90011-6
- Brooks, R.H., and A.T. Corey. 1964. Hydraulic properties of porous media. *Hydrology Papers*, Colorado State University, Ft. Collins, CO.
- Castellini, M., M. Iovino, M. Pirastu, M. Niedda, and V. Bagarello. 2016. Use of BEST procedure to assess soil physical quality in the Baratz Lake Catchment (Sardinia, Italy). *Soil Sci. Soc. Am. J.* 80:742–755. doi:10.2136/sssaj2015.11.0389
- Constantz, J., W. Herkelrath, and F. Murphy. 1988. Air encapsulation during infiltration. *Soil Sci. Soc. Am. J.* 52:10–16. doi:10.2136/sssaj1988.03615995005200010002x
- Fuentes, C., R. Haverkamp, and J.Y. Parlange. 1992. Parameter constraints on closed-form soilwater relationships. *J. Hydrol.* 134:117–142. doi:10.1016/0022-1694(92)90032-Q
- Haverkamp, R., P.J. Ross, K.R.J. Smettem, and J.Y. Parlange. 1994. Three-dimensional analysis of infiltration from the disc infiltrometer: 2. Physically based infiltration equation. *Water Resour. Res.* 30:2931–2935. doi:10.1029/94WR01788
- Klute, A. and C. Dirksen. 1986. Hydraulic conductivity and diffusivity: Laboratory methods. In: A. Klute, editor, *Methods of soil analysis: Part I.* Agron. Monogr. 9. ASA and SSSA, Madison, WI. p. 687–734.
- Lassabatère, L., R. Angulo-Jaramillo, J.M. Soria Ugalde, R. Cuenca, I. Braud, and R. Haverkamp. 2006. Beerkan estimation of soil transfer parameters through infiltration experiments—BEST. *Soil Sci. Soc. Am. J.* 70:521–532. doi:10.2136/sssaj2005.0026
- Reynolds, W., and D. Elrick. 1990. Ponded infiltration from a single ring: I. Analysis of steady flow. *Soil Sci. Soc. Am. J.* 54:1233–1241. doi:10.2136/sssaj1990.03615995005400050006x
- Reynolds, W.D., B.T. Bowman, R.R. Brunke, C.F. Drury, and C.S. Tan. 2000. Comparison of tension infiltrometer, pressure infiltrometer, and soil core estimates of saturated hydraulic conductivity. *Soil Sci. Soc. Am. J.* 64:478–484. doi:10.2136/sssaj2000.642478x
- Scotter, D., B. Clothier, and E. Harper. 1982. Measuring saturated hydraulic conductivity and sorptivity using twin rings. *Soil Res.* 20:295–304. doi:10.1071/SR9820295
- Simunek, J. and M. Sejna. 2011. The HYDRUS software package for simulating the two- and three-dimensional movement of water, heat, and multiple solutes in variably-saturated media. User manual. PC Progress, Prague, Czech Republic.
- Smiles, D.E., and J.H. Knight. 1976. A note on the use of the Philip infiltration equation. *Soil Res.* 14:103–108. doi:10.1071/SR9760103
- Stewart, R.D., and M.R. Abou Najm. 2018. A comprehensive model for single ring infiltration I: Initial water content and soil hydraulic properties. *Soil Sci. Soc. Am. J.* 82: doi: 10.2136/sssaj2017.09.0313
- Stewart, R.D., M.R. Abou Najm, D.E. Rupp, J.W. Lane, H.C. Uribe, J.L. Arumi, et al. 2015. Hillslope runoff thresholds with shrink-swell clay soils. *Hydrol. Processes* 29:557–571. doi:10.1002/hyp.10165
- Stewart, R.D., M.R. Abou Najm, D.E. Rupp, and J.S. Selker. 2016. Modeling multidomain hydraulic properties of shrink-swell soils. *Water Resour. Res.* 52:7911–7930.
- Stewart, R.D., D.E. Rupp, M.R.A. Najm, and J.S. Selker. 2013. Modeling effect of initial soil moisture on sorptivity and infiltration. *Water Resour. Res.* 49:7037–7047. doi:10.1002/wrcr.20508
- Thomas, S.K., J.F. Conta, E.D. Severson, and J.M. Galbraith. 2016. Measuring saturated hydraulic conductivity in soil. Virginia Cooperative Extension, Blacksburg, VA.
- Vandervaere, J.P., C. Peugeot, M. Vauclin, R. Angulo Jaramillo, and T. Lebel. 1997. Estimating hydraulic conductivity of crusted soils using disc infiltrometers and minitensiometers. *J. Hydrol.* 188-189:203–223. doi:10.1016/S0022-1694(96)03160-5
- Vandervaere, J.P., M. Vauclin, and D.E. Elrick. 2000. Transient flow from tension infiltrometers I. The two-parameter equation. *Soil Sci. Soc. Am. J.* 64:1263–1272. doi:10.2136/sssaj2000.6441263x
- Wu, L., L. Pan, J. Mitchell, and B. Sanden. 1999. Measuring saturated hydraulic conductivity using a generalized solution for single-ring infiltrometers. *Soil Sci. Soc. Am. J.* 63:788–792. doi:10.2136/sssaj1999.634788x